

## MICROLENS OGLE-2005-BLG-169 IMPLIES THAT COOL NEPTUNE-LIKE PLANETS ARE COMMON

A. GOULD,<sup>1,2</sup> A. UDALSKI,<sup>3,4</sup> D. AN,<sup>1,2</sup> D. P. BENNETT,<sup>5,6,7</sup> A.-Y. ZHOU,<sup>8</sup> S. DONG,<sup>1,2</sup> N. J. RATTENBURY,<sup>5,9</sup> B. S. GAUDI,<sup>1,10</sup>  
P. C. M. YOCK,<sup>5,11</sup> I. A. BOND,<sup>5,12</sup> G. W. CHRISTIE,<sup>1,13</sup> K. HORNE,<sup>6,14,15</sup> J. ANDERSON,<sup>16</sup> K. Z. STANEK,<sup>1,2</sup>  
D. L. DEPOY,<sup>1,2</sup> C. HAN,<sup>1,17</sup> J. MCCORMICK,<sup>1,18</sup> B.-G. PARK,<sup>1,19</sup> R. W. POGGE,<sup>1,2</sup> S. D. POINDEXTER,<sup>1,2</sup> I. SOSZYŃSKI,<sup>3,4,20</sup>  
M. K. SZYMAŃSKI,<sup>3,4</sup> M. KUBIAK,<sup>3,4</sup> G. PIETRZYŃSKI,<sup>3,4,20</sup> O. SZEWczyk,<sup>3,4</sup> Ł. WYRZYKOWSKI,<sup>3,4,21</sup> K. ULACZYK,<sup>3,4</sup>  
B. PACZYŃSKI,<sup>3,22</sup> D. M. BRAMICH,<sup>6,14,21</sup> C. SNODGRASS,<sup>14,23</sup> I. A. STEELE,<sup>14,24</sup> M. J. BURGDORF,<sup>14,24</sup>  
M. F. BODE,<sup>14,24</sup> C. S. BOTZLER,<sup>5,11</sup> S. MAO,<sup>9</sup> AND S. C. SWAVING<sup>5,11</sup>

Received 2006 March 10; accepted 2006 April 27; published 2006 May 24

### ABSTRACT

We detect a Neptune mass ratio ( $q \approx 8 \times 10^{-5}$ ) planetary companion to the lens star in the extremely high magnification ( $A \sim 800$ ) microlensing event OGLE-2005-BLG-169. If the parent is a main-sequence star, it has mass  $M \sim 0.5 M_{\odot}$ , implying a planet mass of  $\sim 13 M_{\oplus}$  and projected separation of  $\sim 2.7$  AU. When intensely monitored over their peak, high-magnification events similar to OGLE-2005-BLG-169 have nearly complete sensitivity to Neptune mass ratio planets with projected separations of 0.6–1.6 Einstein radii, corresponding to 1.6–4.3 AU in the present case. Only two other such events were monitored well enough to detect Neptunes, and so this detection by itself suggests that Neptune mass ratio planets are common. Moreover, another Neptune was recently discovered at a similar distance from its parent star in a low-magnification event, which are more common but are individually much less sensitive to planets. Combining the two detections yields 90% upper and lower frequency limits  $f = 0.38_{-0.22}^{+0.31}$  over just 0.4 decades of planet-star separation. In particular,  $f > 16\%$  at 90% confidence. The parent star hosts no Jupiter-mass companions with projected separations within a factor 5 of that of the detected planet. The lens-source relative proper motion is  $\mu \sim 7\text{--}10$  mas yr<sup>-1</sup>, implying that if the lens is sufficiently bright,  $I \lesssim 23.8$ , it will be detectable by the *Hubble Space Telescope* by 3 years after peak. This would permit a more precise estimate of the lens mass and distance and, so, the mass and projected separation of the planet. Analogs of OGLE-2005-BLG-169Lb orbiting nearby stars would be difficult to detect by other methods of planet detection, including radial velocities, transits, and astrometry.

*Subject headings:* Galaxy: bulge — gravitational lensing — planetary systems

The regions of our solar system beyond Mars contain giant planets, as well as asteroids and comets—which are believed to be remnants of the process that formed these bodies—and also moons, which may serve as analogs to bodies involved in the late stages of planet formation. However, despite some 170 planet discoveries over the past decade, the analogous regions around other mature stars remain relatively inaccessible

to us. As radial velocity (RV) survey time baselines have grown, they have begun to detect gas giants in these regions, but RV is sensitive to Neptune-mass planets only when they are much closer to their parent stars. Transit surveys are even more heavily biased toward close-in planets. Astrometric sensitivity does peak at large orbits but is fundamentally restricted to orbital periods that are shorter than the survey.

<sup>1</sup> Microlensing Follow-up Network ( $\mu$ FUN).

<sup>2</sup> Department of Astronomy, Ohio State University, 140 West 18th Avenue, Columbus, OH 43210; gould@astronomy.ohio-state.edu.

<sup>3</sup> Optical Gravitational Lensing Experiment (OGLE).

<sup>4</sup> Obserwatorium Astronomiczne Uniwersytetu Warszawskiego, Aleje Ujazdowskie 4, 00-478 Warsaw, Poland; udalski@astrouw.edu.pl.

<sup>5</sup> Microlensing Observations in Astrophysics (MOA) Collaboration.

<sup>6</sup> Probing Lensing Anomalies NETwork (PLANET) Collaboration.

<sup>7</sup> Department of Physics, 225 Nieuwland Science Hall, Notre Dame University, Notre Dame, IN 46556.

<sup>8</sup> Department of Physics, Astronomy, and Materials Science, Missouri State University, 901 South National Avenue, Springfield, MO 65897.

<sup>9</sup> Jodrell Bank Observatory, University of Manchester, Macclesfield, Cheshire SK11 9DL, UK.

<sup>10</sup> Harvard-Smithsonian Center for Astrophysics, 60 Garden Street, Cambridge, MA 02138.

<sup>11</sup> Department of Physics, University of Auckland, Private Bag 92-019, Auckland 1001, New Zealand.

<sup>12</sup> Institute for Information and Mathematical Sciences, Massey University, Private Bag 102-904, Auckland 1330, New Zealand.

<sup>13</sup> Auckland Observatory, P.O. Box 24-180, Auckland, New Zealand.

<sup>14</sup> RoboNet Collaboration.

<sup>15</sup> Scottish Universities Physics Alliance, School of Physics and Astronomy, University of St. Andrews, North Haugh, St. Andrews KY16 9SS, UK.

<sup>16</sup> Department of Physics and Astronomy, MS-108, Rice University, 6100 Main Street, Houston, TX 77005.

<sup>17</sup> Department of Physics, Institute for Basic Science Research, Chungbuk National University, Chongju 361-763, South Korea.

<sup>18</sup> Farm Cove Observatory, Center for Backyard Astrophysics, 2/24 Rapallo Place, Pakuranga, Auckland 1706, New Zealand.

By contrast, microlensing sensitivity peaks at the Einstein ring, which is typically at 2–4 AU, depending on the mass and distance of the host star, and it extends several times farther out. Moreover, microlensing detections are “instantaneous snapshots” of the system, not requiring an orbital period to elapse. Hence, microlensing can potentially yield important information about the intermediate-to-outer regions of extrasolar planetary systems that are difficult to probe by other techniques.

Gravitational microlensing occurs when a “lens” star becomes closely aligned, within an angular Einstein radius  $\theta_E$ , with a more distant source star. The source is magnified by an amount that grows monotonically as it approaches the lens and diverges inversely with separation for extremely close encounters (Einstein 1936; Paczyński 1986).

Planets hosted by the lens star induce two, generally distinct, perturbations on the single-lens magnification pattern: a small

<sup>19</sup> Korea Astronomy and Space Science Institute, Hwaam-dong, Yuseong-gu, Daejeon 305-348, South Korea.

<sup>20</sup> Departamento de Física, Universidad de Concepción, Casilla 160-C, Concepción, Chile.

<sup>21</sup> Institute of Astronomy, University of Cambridge, Madingley Road, Cambridge CB3 0HA, UK.

<sup>22</sup> Princeton University Observatory, Peyton Hall, Princeton, NJ 08544.

<sup>23</sup> Astrophysics Research Centre, Department of Physics and Astronomy, Queen’s University Belfast, University Road, Belfast BT7 1NN, UK.

<sup>24</sup> Astrophysics Research Institute, Liverpool John Moores University, Twelve Quays House, Egerton Wharf, Birkenhead CH41 1LD, UK.

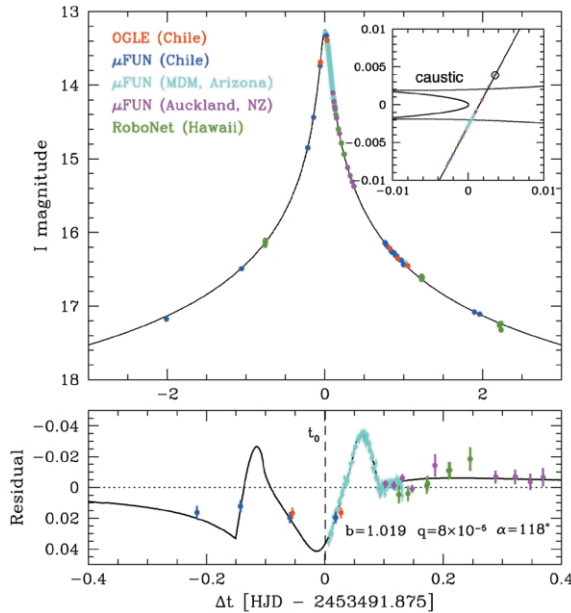


FIG. 1.—*Top*: Data and best-fit model for OGLE-2005-BLG-169. *Bottom*: Difference between this model and a single-lens model with the same  $(t_0, u_0, t_E, \rho)$ . It displays the classical form of a caustic entrance/exit that is often seen in binary microlensing events, where the amplitudes and timescales are several orders of magnitude larger than seen here. MDM data trace the characteristic slope change at the caustic exit ( $\Delta t = 0.092$ ) extremely well, while the entrance is tracked by a single point ( $\Delta t = -0.1427$ ). The dashed line indicates the time  $t_0$ . *Inset*: Source path through the caustic geometry. The source size  $\rho$  is indicated.

“planetary caustic” (closed contour of formally infinite magnification) directly associated with the planet, and an even smaller “central caustic” closely aligned with the host. All microlensing events have the potential to probe the planetary caustic, but owing to its small extent and the random trajectory of the source, the probability for the source to encounter the perturbed region is low.

By contrast, the small fraction of events that reach very high magnification (and thus small lens-source separation) *automatically* probe the region of the central caustic (Griest & Safizadeh 1998; Rhie et al. 2000; Bond et al. 2002; Rattenbury et al. 2002). Hence, even low-mass planets lying anywhere sufficiently near the Einstein ring are virtually guaranteed to perturb the light curve (Abe et al. 2004). Since the peak of the event can, at least in principle, be predicted in advance, it is possible to focus limited observing resources to make the intensive observations over the peak that are required to detect and characterize the relatively subtle signal.

The  $\mu$ FUN team has adopted a strategy of trying to recognize the few prospective high-magnification events among the roughly 500 microlensing events annually alerted by the OGLE-III Early Warning System (Udalski 2003) and the roughly 50 events annually alerted by the MOA Collaboration. During the 2005 season, this strategy led to the discovery of two planets. The first was the Jovian mass ratio OGLE-2005-BLG-071Lb (Udalski et al. 2005). Here we report the second such planet, a Neptune mass ratio companion to the lens in OGLE-2005-BLG-169.

On 2005 April 21, the OGLE Collaboration alerted OGLE-2005-BLG-169 as probable microlensing of a faint ( $I = 19.4$ ) source toward the Galactic bulge, using the 1.3 m Warsaw telescope in Chile (operated by the Carnegie Institution of Washington). After observations by OGLE and the 1.3 m  $\mu$ FUN SMARTS telescope in Chile showed the event to be of extremely high magnification, the observers at the 2.4 m  $\mu$ FUN MDM telescope in Arizona interrupted their regular program to obtain

more than 1000 exposures over the peak. Additional data come from the 0.35 m  $\mu$ FUN Nustrini Telescope in Auckland, New Zealand, and the 2.0 m PLANET/RoboNet Faulkes Telescope North in Hawaii. We analyze a total of 340, 22, 1025, 74, and 31 images with typical exposure times of 120, 300, 10, 120, and 100 s in the  $I, I, I, \text{clear},$  and  $R$  passbands, respectively, from these five telescopes. In addition, six  $V$ -band images from  $\mu$ FUN SMARTS permit determination of the source color.

All data were reduced using the OGLE data pipeline, based on difference imaging analysis (DIA; Woźniak 2000). The  $\mu$ FUN MDM data were also reduced using the ISIS pipeline (Alard & Lupton 1998; Alard 2000; Hartman et al. 2004). To test for any systematics in this crucial data set, we report results below derived from these two completely independent pipelines.

Planets are discovered in microlensing events from the brief perturbation they induce on a single-lens light curve (Mao & Paczyński 1991; Gould & Loeb 1992):  $F(t) = F_s A(u(t)) + F_b$ , where  $A(u) = (u^2 + 2)/u(u^2 + 4)^{1/2}$ ,  $u(t) = (\tau^2 + u_0^2)^{1/2}$ , and  $\tau = (t - t_0)/t_E$ . Here  $F(t)$  is the observed flux,  $F_s$  is the source flux,  $F_b$  is flux due to any unlensed background light,  $A$  is the magnification, and  $\mathbf{u} = (\tau, u_0)$  is the vector position of the source normalized to  $\theta_E$ , expressed in terms of the three geometric parameters of the event: the time of closest approach  $t_0$ , the normalized impact parameter  $u_0$ , and the Einstein timescale  $t_E$ .

To describe the planetary perturbation, three “binary lens” parameters are required in addition to the three single-lens geometric parameters (with conventions defined in Udalski et al. 2005)  $t_0$ ,  $u_0$ , and  $t_E$ . These are the binary mass ratio,  $q$ , the separation of the components (in units of  $\theta_E$ ),  $b$ , and angle of the source trajectory relative to the binary axis,  $\alpha$ . Finally, a seventh parameter,  $\rho \equiv \theta_*/\theta_E$ , is required whenever the angular radius of the source  $\theta_*$  plays a significant role, in particular, whenever the source crosses a caustic.

For planetary lenses with caustic crossings, there are seven directly observable and pronounced light-curve features that directly constrain the seven model parameters, up to a well-understood twofold degeneracy (Dominik 1999) that takes  $b \leftrightarrow b^{-1}$ . Three of these, the epoch, duration, and height of the primary lensing event, strongly constrain  $(t_0, t_E, u_0)$ . The other four, the two caustic-crossing times (entrance and exit) and the height and duration of one of the caustic crossings, then constrain  $(b, q, \alpha, \rho)$ .

As we now show, OGLE-2005-BLG-169 is indeed a caustic-crossing event. However, only the caustic exit (and not entrance) was well resolved. This leads to a one-dimensional degeneracy among the model parameters, which is then partially broken by secondary, less pronounced, features of the light curve.

The residuals to the single-lens models shown in Figure 1 exhibit a kink in slope at  $\Delta t = 0.092$  days, where  $\Delta t$  is the time elapsed since HJD 2,453,491.875 (2005 May 1, UT 09:00). The kink is equally apparent in both sets of MDM reductions. While the *incident slope* of this kink in the light curve depends on the particular single-lens model used, the *slope discontinuity* is model independent. Such a change in slope is induced by a caustic exit, when the trailing limb of the source crosses the caustic, causing two of its images to merge and finally vanish.

To extract model parameters, we undertake a brute-force search of parameter space. We hold the three parameters  $b$ ,  $\alpha$ , and  $q$  fixed at a grid of values while minimizing  $\chi^2$  over the remaining four parameters, using the values of  $t_0$ ,  $u_0$ , and  $t_E$  derived from the overall shape of the light curve as seeds. We find two distinct local minima that obey the  $b \leftrightarrow b^{-1}$  degeneracy. These minima are embedded in elongated  $\Delta\chi^2$  valleys (Fig. 2), with  $[\alpha(\text{radians}) : b]$  axis ratio  $\sim 100$ , which occur because there are only six pronounced features in the light curve to constrain seven model parameters. However, while the caustic entrance

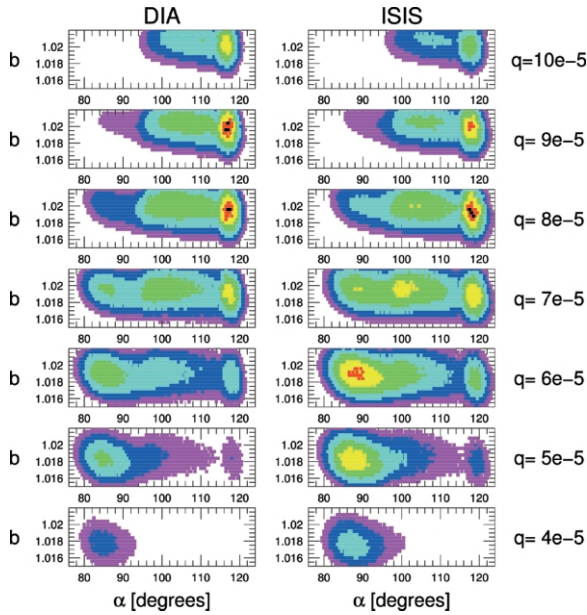


FIG. 2.— $\Delta\chi^2$  contours relative to the respective minima for light-curve fits using the DIA and ISIS reductions of the MDM data;  $\sigma \equiv (\Delta\chi^2)^{1/2} < 1, 2, 3, 4, 5, 6,$  and  $7$  are shown by black, red, yellow, green, cyan, blue, and magenta, respectively. Note that the abscissae are compressed, so the  $6\sigma$  contours have an axis ratio of approximately 100 (with  $\alpha$  expressed in radians), which reflects the one-dimensional degeneracy discussed in the text. Both reductions have their minimum at  $(\alpha, q) \sim (120^\circ, 8 \times 10^{-5})$ . Similar contours for  $b < 1$  yield additional solutions that are included in Table 1. The full  $3\sigma$  mass ratio range is confined to  $(5\text{--}10) \times 10^{-5}$ , even allowing for both reductions.

is not well resolved, the point at  $\Delta t = -0.1427$  days does lie on this entrance and thereby singles out the solutions shown in Table 1. Nevertheless, to be conservative, we quote  $3\sigma$  errors for light-curve parameters, which take account of both the elongated valleys and the two reductions. Most importantly,

$$q = 8_{-3}^{+2} \times 10^{-5}, \quad b = 1.00 \pm 0.02 \quad (3\sigma).$$

In microlensing events, the physical parameters (lens mass  $M$ , lens-source relative parallax  $\pi_{\text{rel}}$ , and relative proper motion  $\mu$ ) are related to the “observable” event parameters ( $t_E$ ,  $\theta_E$ , and the microlens parallax  $\pi_E$ ) by  $\theta_E = (\kappa M \pi_{\text{rel}})^{1/2}$ ,  $\pi_E = (\kappa M / \pi_{\text{rel}})^{1/2}$ , and  $t_E = \theta_E / \mu$ , where  $\kappa \equiv 4G/(c^2 \text{ AU})$ . Of these, only  $t_E$  is routinely measurable. However, in caustic-crossing events, one can usually also measure  $\theta_E$ , which both directly constrains the mass-distance relation and yields a measurement of  $\mu$ . We first determine the angular source radius  $\theta_*$  using the standard approach (Yoo et al. 2004), finding  $\theta_* = 0.44 \pm 0.04 \mu\text{as}$ . Together with the parameter measurements  $\rho = 4.4_{-0.6}^{+0.9} \times 10^{-4}$  and  $t_E = 43 \pm 4$  days, this yields  $3\sigma$  ranges

$$\theta_E = \theta_* / \rho = 1.00 \pm 0.22 \text{ mas},$$

$$\mu = \theta_E / t_E = 8.4 \pm 1.7 \text{ mas yr}^{-1}.$$

Another constraint comes from the upper limit on the lens flux, which cannot exceed the background flux measurement  $F_b$  (corresponding to  $I_b = 19.8$ ). We also derive from the light curve a weak constraint on the microlens parallax,  $\pi_{E,\parallel} = -0.086 \pm 0.261$ , which we include for completeness. Here  $\pi_{E,\parallel} \equiv \pi_E \cos \psi$ , where  $\psi$  is the angle between the direction of lens-source relative motion and the position of the Sun at  $t_0$  projected on the plane of the sky (Gould 2004).

These measurements, together with a Bayesian prior for the lens distances and masses from a Han & Gould (2003) Galaxy model and Gould (2000) mass function (but with a Salpeter  $[-2.35]$  slope at the high end), together with the assumption that all stellar objects along the line of sight are equally likely to harbor planets (since there is no prior information on planet frequency as a function of stellar properties for Neptune-mass extrasolar planets beyond 1 AU), yield a probability distribution for the lens mass. We find that the probabilities that the lens is a main-sequence star (MS), white dwarf (WD), neutron star (NS), and black hole (BH) are respectively 55%, 32%, 11%, and 2%. However, Neptune mass ratio planets around NSs must be quite rare, because the  $\sim 0.2$  s oscillations they induce would easily show up in pulsar timing residuals. Since BHs and NSs form by a similar process, this may also argue against BHs as the host. MSs and WDs represent different life stages of the same class of stars. If the host is a MS, then the median and 90% confidence interval for the mass and distance are given by

$$M = 0.49_{-0.29}^{+0.23} M_\odot, \quad D_L = 2.7_{-1.3}^{+1.6} \text{ kpc} \quad (90\% \text{ confidence}),$$

implying that the best estimates for the planet mass and separation are  $m_p = qM \sim 13 M_\oplus$  and  $r_\perp = b\theta_E D_L \sim 2.7$  AU, where  $D_L$  is the distance to the lens. If the lens is a WD, the 90% confidence mass and distance distributions are similar,  $M = 0.56_{-0.14}^{+0.39} M_\odot$  and  $D_L = 3.1_{-0.9}^{+1.5}$  kpc, and hence the corresponding planet characteristics are also similar. Future observations by the *Hubble Space Telescope* could distinguish between MS and WD hosts, as well as measuring the mass and distance of the former provided that the lens is brighter than  $I \sim 23.8$  (D. P. Bennett & J. Anderson 2006, in preparation).

Does lens OGLE-2005-BLG-169L have planets other than OGLE-2005-BLG-169Lb? Central caustic events allow one to address this question because all the companions to the lens star perturb the central caustic (Gaudi et al. 1998). Moreover, the combined perturbation from two planets is very nearly the sum of the separate perturbations, unless the two planets are closely aligned (Rattenbury et al. 2002; Han 2005). This allows us to subtract the perturbation from the one detected planet and apply the same search technique to the resulting (nearly single-lens) light curve to look for others. We find none and so place upper limits on the presence of other planets. In particular, we exclude Jupiter-mass planets ( $q = 2 \times 10^{-3}$ ) at projected separations within a factor of 5.5 of the Einstein radius ( $0.18 < b < 5.5$ ) and Saturn-mass planets within a factor of 3.5.

TABLE 1  
LIGHT-CURVE MODELS

Pipeline	$\Delta\chi^2$	$t_0 - t_{\text{ref}}$ (days)	$u_0$ ( $\times 10^3$ )	$t_E$ (days)	$b$	$q$ ( $\times 10^5$ )	$\alpha$ (deg)	$\rho$ ( $\times 10^4$ )	$\theta_E$ (mas)	$\mu$ (mas yr $^{-1}$ )
DIA .....	0.00	0.0008	1.24	42.27	1.0198	8.6	117.0	4.4	1.00	8.6
ISIS .....	0.00	0.0009	1.23	42.56	1.0194	8.2	118.2	4.7	0.93	8.0
DIA .....	0.27	0.0004	1.25	42.09	0.9819	8.3	122.6	3.9	1.12	9.7
ISIS .....	2.33	0.0007	1.17	44.69	0.9825	7.3	123.5	4.0	1.11	9.0

NOTE.—Here  $t_{\text{ref}} = \text{HJD } 2,453,491.875$  (2005 May 1, UT 09:00).

OGLE-2005-BLG-169 is one of only three extremely high magnification events with sensitivity to the central caustics induced by cold Neptunes, the other two being MOA-2003-BLG-32/OGLE-2003-BLG-219 and OGLE-2004-BLG-343 (Abe et al. 2004; Dong et al. 2006). The probabilities that a  $q = 8 \times 10^{-5}$  planet lying at random projected position in the “lensing zone” ( $0.6 < b < 1.6$ ) for these three events are 100%, 85%, and 40%, respectively. This implies  $\langle f \rangle = 1/2.25 = 44\%$  for the expected fraction of stars hosting cold Neptunes within the lensing zone (0.4 decades of projected separation), but with very large uncertainty due to small number statistics.

However, we can improve our estimate by incorporating the detection of OGLE-2005-BLG-390Lb, which is a very similar ( $b = 1.6$ ,  $q = 7.6 \times 10^{-5}$ ) planet that was detected through the other (planetary caustic) microlensing channel (Beaulieu et al. 2006). The expected number of detections of  $q = 8 \times 10^{-5}$  lensing-zone planets (through this planetary caustic channel) was  $1.75f$  for 1995–1999 (Gaudi et al. 2002). We estimate that the expected number for 2000–2005 is a factor of 1.5 higher based on a comparison of the survey characteristics during these two periods. Hence, the single detection through this channel yields  $\langle f \rangle = 23\%$ , also with large errors. If we combine the two channels and impose a uniform prior, we find a median and 90% upper and lower limits of  $f = 0.38^{+0.31}_{-0.22}$ , in particular, a 90% confidence lower limit of  $f > 16\%$ . This result is robust to possible errors in our estimate of sensitivity of the 2000–2005 surveys. If the factor of 1.5 is changed to 1.0 or 2.0 (our estimate of the full plausible range), the lower limit changes only by 2%, from 16% to 18% or 14%, respectively.

Figure 3 addresses the question how well analogs of OGLE-2005-BLG-169Lb (with the same mass ratio and semimajor axis) can be detected by other planet-search techniques. At its projected separation, it lies well below the mass sensitivity of RV surveys. Its semimajor axis places it well beyond the reach of a space-based transit mission such as *Kepler*. Only the future astrometric *SIM PlanetQuest* can potentially probe these cold Neptunes.

Both OGLE-2005-BLG-169Lb and OGLE-2005-BLG-390Lb are in the cold outer regions of their planetary systems, with expected surface temperatures of  $\sim 70$  and  $\sim 50$  K, corresponding roughly to the environments of Saturn and Neptune, respectively. Both have Neptune/Sun mass ratios, with median absolute mass estimates of 13 and  $6 M_{\oplus}$ , respectively. They must have a large fraction of rock and ice, but whether these are covered with a thick coat of gas, like Uranus and Neptune, or whether they are “naked” super-Earths such as are theorized to have formed the cores of Jupiter and Saturn, is unclear. If such cores formed routinely but usually failed to accrete the ambient gas before it dispersed, this would account for the high frequency of these objects (Ida & Lin 2005). Moreover, the absence of gas giants within a factor of 5.5 of OGLE-2005-BLG-169’s Einstein ring is consistent

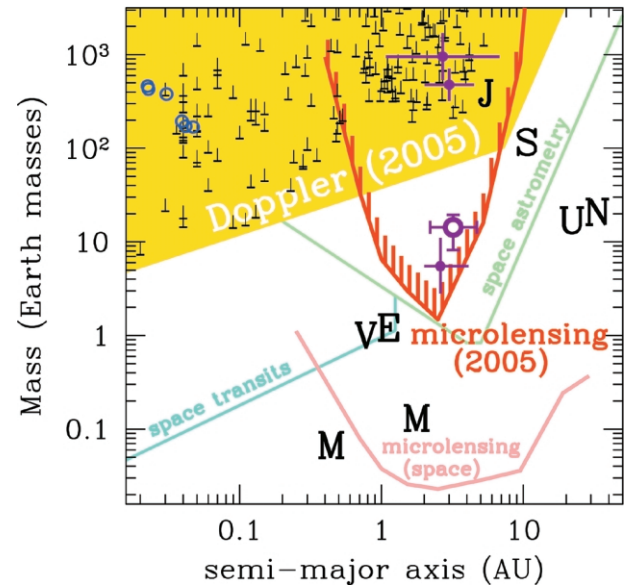


FIG. 3.—Exoplanet discovery potential and detections as functions of planet mass and semimajor axis. Potential is shown for current ground-based RV (yellow) and, very approximately, microlensing (red) experiments, as well as future space-based transit (cyan), astrometric (green), and microlensing (peach) missions. Planets discovered using the transit (blue), RV (black), and microlensing (magenta) techniques are shown as individual points, with OGLE-2005-BLG-169Lb displayed as an open symbol. Solar system planets are indicated by their initials for comparison.

with the idea that the detected planet is such a “failed Jupiter” (Laughlin et al. 2004). One could gain further clues by mapping out the mass and separation distributions of a larger sample.

We acknowledge the following support: NSF AST 04-52758 (A. G., S. D.); NASA NNG04GL51G (D. L. D., A. G., R. W. P.); Polish MEIN 2P03D02124, NSF AST 02-04908, NASA grant NAG 5-12212 (OGLE); Polish FNP SP13/2003 (A. U.); NSF AST 02-06189, NASA NAF 5-13042 (D. P. B.); NSF AST 03-07480 (A.-Y. Z.); Menzel Fellowship, Harvard College Observatory (B. S. G.); SRC Korea Science and Engineering Foundation (C. H.); the Korea Astronomy and Space Science Institute (B.-G. P.); Marsden Fund of New Zealand (I. A. B., P. C. M. Y.); the Deutsche Forschungsgemeinschaft (C. S. B.); PPARC, EU FP6 program “ANGLES” (Ł. W., S. M., N. J. R.); PPARC (RoboNet); and the Dill Faulkes Educational Trust (Faulkes Telescope North). Assistance by Lydia Philpott, Jan Snigula, and the computer science department of the University of Auckland is acknowledged. We thank the MDM staff for their support. All findings are those of the authors and do not necessarily reflect NSF views.

#### REFERENCES

- Abe, F., et al. 2004, *Science*, 305, 1264  
 Alard, C. 2000, *A&AS*, 144, 363  
 Alard, C., & Lupton, R. H. 1998, *ApJ*, 503, 325  
 Beaulieu, J.-P., et al. 2006, *Nature*, 439, 437  
 Bond, I. A., et al. 2002, *MNRAS*, 331, L19  
 Dominik, M. 1999, *A&A*, 349, 108  
 Dong, S., et al. 2006, *ApJ*, 642, 842  
 Einstein, A. 1936, *Science*, 84, 506  
 Gaudi, B. S., Naber, R. M., & Sackett, P. D. 1998, *ApJ*, 502, L33  
 Gaudi, B. S., et al. 2002, *ApJ*, 566, 463  
 Gould, A. 2000, *ApJ*, 535, 928  
 ———. 2004, *ApJ*, 606, 319  
 Gould, A., & Loeb, A. 1992, *ApJ*, 396, 104  
 Griest, K., & Safizadeh, N. 1998, *ApJ*, 500, 37  
 Han, C. 2005, *ApJ*, 629, 1102  
 Han, C., & Gould, A. 2003, *ApJ*, 592, 172  
 Hartman, J. D., Bakos, G., Staneck, K. Z., & Noyes, R. W. 2004, *AJ*, 128, 1761  
 Ida, S., & Lin, D. N. C. 2005, *ApJ*, 626, 1045  
 Laughlin, G., Bodenheimer, P., & Adams, F. C. 2004, *ApJ*, 612, L73  
 Mao, S., & Paczyński, B. 1991, *ApJ*, 374, L37  
 Paczyński, B. 1986, *ApJ*, 304, 1  
 Rattenbury, N. J., Bond, I. A., Skuljan, J., & Yock, P. C. M. 2002, *MNRAS*, 335, 159  
 Rhie, S. H., et al. 2000, *ApJ*, 533, 378  
 Udalski, A. 2003, *Acta Astron.*, 53, 291  
 Udalski, A., et al. 2005, *ApJ*, 628, L109  
 Woźniak, P. R. 2000, *Acta Astron.*, 50, 421  
 Yoo, J., et al. 2004, *ApJ*, 603, 139